Nucleation-Limited Dewetting of Ice Films on Pt(111)

Konrad Thürmer and Norman C. Bartelt
Sandia National Laboratories, Livermore, California 94550, USA
(Received 18 December 2007; published 6 May 2008)

Quantifying dewetting phenomena at the microscopic level is the key to deciphering how a balance between kinetic and equilibrium effects determines ice-film morphology on Pt(111). Overcoming the difficulty of imaging nominally insulating ice multilayers with scanning tunneling microscopy allowed us to track the dewetting process. The results show that the rate at which new layers nucleate, and not surface diffusion, determines how fast individual crystallite shapes equilibrate. Applying nucleation theory to measured growth rates versus crystallite size, we obtain new bounds on the energetics both of step formation on ice and of the Pt-ice interface.

DOI: 10.1103/PhysRevLett.100.186101 PACS numbers: 68.55.−a, 64.60.qj, 68.37.Ef, 68.43.Hn

The nucleation of ice on solid substrates is important in many natural phenomena [1,2]. For example, rainfall is triggered by nucleation of ice crystals on micron-sized particles in clouds. Still, very little is known about the early stages of ice growth at the molecular level. The nature of water molecule-substrate interactions is still controversial [3], for example.

A direct way to study nucleation phenomena on metal and semiconductor surfaces is scanning tunneling microscopy (STM). But, because ice is an electrical insulator, imaging thick ice films nondestructively is difficult with STM [4,5]. Several STM studies [4,6,7] of the growth of the first one or two layers of ice, at low temperature in UHV, have given insight into the initial stages of growth. Recently small ice crystals evolving from annealed amorphous ice have also been observed [5]. Still, there have been no STM observations tracking the growth of complete multilayers, leaving the basics unknown: How close are the growing crystals to thermal equilibrium? How do new layers nucleate? And how do surface diffusion and substrate-ice interactions affect the evolution of the crystals? Here we report overcoming the problem of imaging ice with STM. We find that with extremely small tunneling current and sufficiently large negative sample biases thick layers of ice can be imaged nondestructively. We use this new capability to investigate how crystalline ice multilayers, grown on Pt(111), evolve.

Thin uniform films are often thermodynamically unstable: they can lower interfacial energy by forming three-dimensional crystals while exposing the substrate or a thin wetting layer. Determining whether dewetting is kinetically hindered, or determining the processes by which it occurs, is crucial to understanding how the morphology of grown films relates to their energetics and equilibrium configuration [8–11]. An example of a heavily studied system, where this question is important, is ice on Pt(111) [12–16]. It is believed that the equilibrium structure comprises isolated three-dimensional ice crystals on a Pt(111) surface covered by a bilayer of water molecules. That is, ice dewets Pt. The processes by which the dewetting occurs are not known. Often, for example, in the dewetting of fluid films, the rate at which atoms diffuse away from the substrate controls the kinetics. Mullins and Rohrer [17] recently pointed out, however, that the shape evolution of freestanding small crystals is often controlled instead by the rate of nucleation of new atomic layers. They, as well as and others [18], demonstrated that because of the large energy cost of creating new step edges, this nucleation barrier can be insurmountable for crystals larger than a few nm, severely limiting their shape equilibration. Because so little is known about step energies on ice, and about surface and interface energies, it is not clear whether the driving force for dewetting is large enough to nucleate the new layers required for ice crystals to grow. New layer nucleation is not observed in dewetting of metal-on-metal films, for example [11]. As reported below, we use STM to monitor the evolution of crystalline multilayer ice films during annealing at 140 K and find that the three-dimensional ice crystals do indeed grow higher by nucleating new ice layers on their top facets, even in the absence of deposition. After recording hundreds of individual nucleation events we compare the rate at which ice layers are added to nucleation theory. The parameters that emerge from the analysis place bounds on the energetics of ice surfaces and interfaces.

The ice films were grown in UHV at a rate of 0.1 nm/min by directing water vapor onto the platinum sample held at 140 K. For imaging, performed at ≈ 120 K, we used a negative sample bias of $V_{\text{sample}} < -6(\pm 1)$ V. Using low tunneling currents of ~ 0.4 pA we do not observe any sign of scanning induced surface changes. This ability to image >3 nm thick ice films is counterintuitive because STM relies on electric conductivity and ice is a good insulator [1]. But our experiments show reproducibly that imaging *is* possible at $V_{\text{sample}} < -6(\pm 1)$ V, whereas at $V_{\text{sample}} > -6(\pm 1)$ V the STM tip collides with the ice film and scatters material across the surface. Since the threshold voltage of $-6(\pm 1)$ V for imaging corresponds to the energy of the first occupied states of ice in contact with Pt

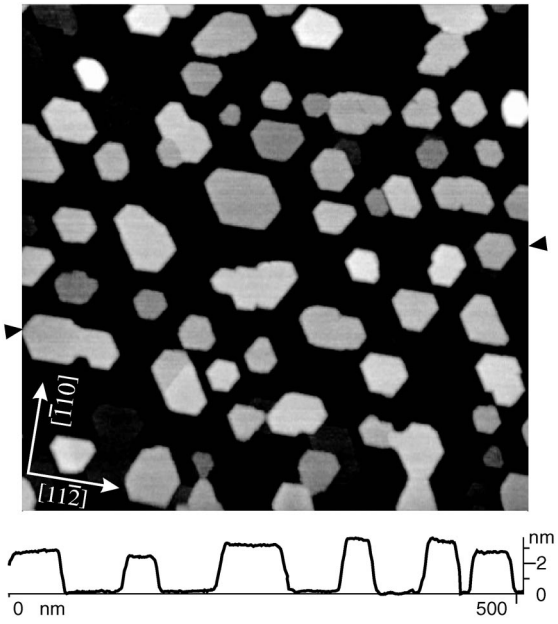

FIG. 1. Surface topography of a crystalline ice-multilayer film on Pt(111). This 500 nm × 500 nm STM image, showing individual ≈ 3 nm high ice crystals grown at 140 K, demonstrates the capability of STM to investigate ice multilayers nondestructively. The height profile displayed below the image was taken along the line connecting the two triangular markers.

[19] it is plausible that the applied voltage lifts the energy levels of the ice sufficiently that electrons can tunnel through the vacuum gap from the highest occupied H_2O orbital into the empty states of the *W* STM tip. (In Ref. [20] we argue the voltage drop across the ice film is small, possibly because of the large polarizability of water.)

Using our imaging capability, we investigated how multilayer ice films dewet the substrate. The typical morphology of ice grown at 140 K, with 1 nm mean thickness, is captured in Fig. 1, and in the larger 1 μm^2 STM image of Fig. 2(a). The film is comprised of individual ≈ 3 nm high crystallites embedded in a one bilayer high wetting layer, consistent with thermal desorption measurements of Kimmel *et al.* [12]. The crystallites have flat top facets and exhibit straight edges along the $\langle 11\bar{2}\rangle$ directions of the substrate. In Ref. [20] we report how the morphology of as-grown films varies with thickness. (For an image of the wetting layer see [21].) That our STM measurements agree well with the film morphology derived from the thermal desorption experiments [12] corroborates that the large electric fields associated with the STM imaging process do not disrupt the film structure.

We find that the ice films tend to dewet the bilayer-covered Pt surface when annealed. The image sequence in Figs. 2(a) and 2(b) reveals that the ice crystals grow thicker to expose more of the bilayer-covered Pt surface. Figure 2(a) shows an image of the starting as-deposited film (1 nm mean thickness grown at 140 K). The height of each crystallite above the wetting layer, in units of bulk-ice bilayer heights, is indicated by shading each crystal ac-

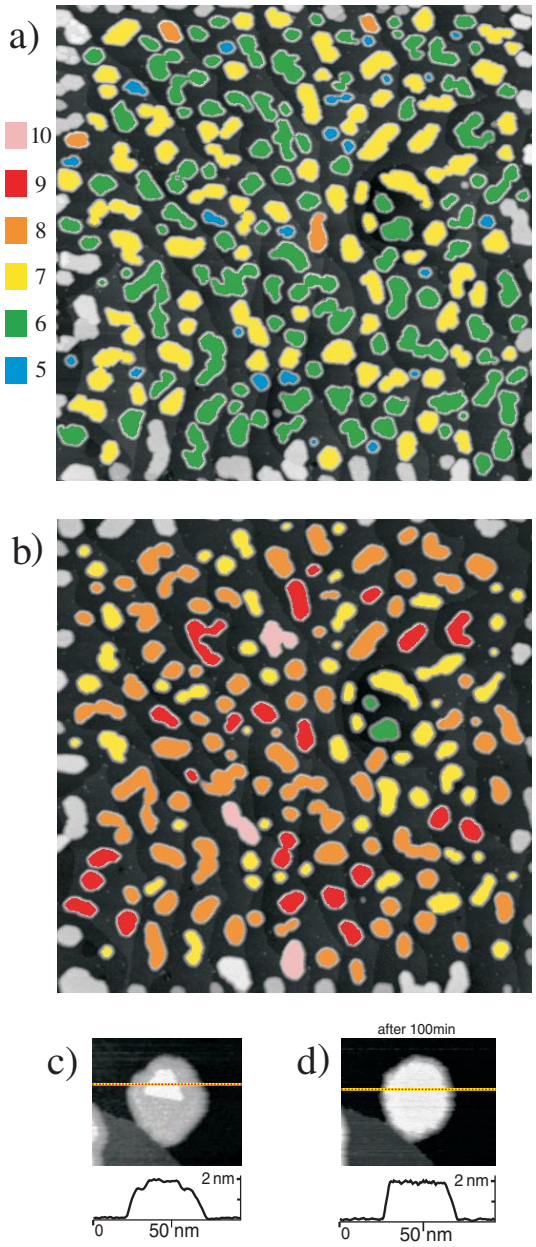

FIG. 2 (color). Nucleation-limited dewetting. (a) 1 μm^2 image of an ice film grown at 140 K with the height of each three-dimensional crystallite colored differently. (b) Image of the same surface region after annealing at 140 K for 1 h. (c),(d) Prior to acquiring ($V_{\text{sample}} = -5$ V, $I_t = 0.35$ pA) these two images, the STM tip was biased at $V_{\text{sample}} = 0.3$ V, and scraped away the uppermost layers of the crystal, reducing its height to 4 bilayers (above wetting layer).

cording to the given color code. As seen in the histogram of Fig. 3(a), the measured crystal heights are quantized around integer bilayer heights. This means the ice crystals grow in discrete jumps of one molecular bilayer, as expected at low temperature. Heating this initial configuration to 140 K for 1 h causes the crystals to grow higher as seen in Fig. 2(b) and the height histograms of Fig. 3(b). The STM tip was retracted during the annealing to avoid tip

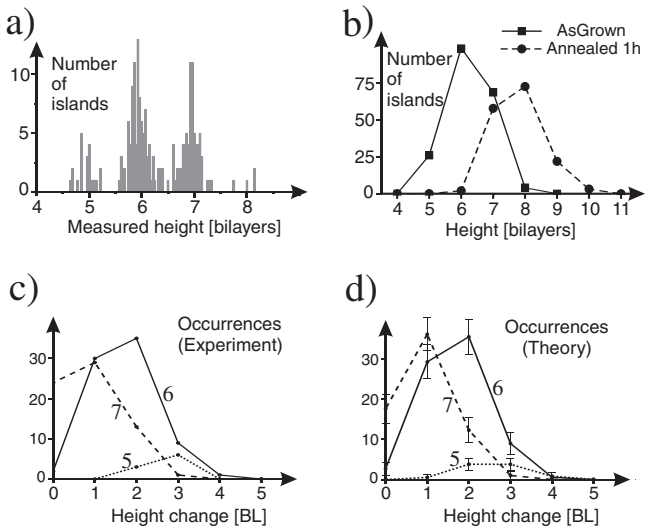

FIG. 3. Analysis of the film evolution upon annealing. (a) Histogram of the average height of each crystallite above the wetting layer showing the discreteness in height. (b) Comparison between the height distributions of the images in Figs. 2(a) and 2(b). (c),(d) Number of crystals of initial height h (labeled for each curve) that have changed in height by n layers. (c) shows the experimental results, (d) shows the numbers predicted from Eq. (2).

induced morphology changes. Since the total ice volume in these images is nearly conserved (i.e., it drops by only $\approx 5\%$, presumably from sublimation), the 30% decrease in area covered by more-than-one-bilayer-thick crystals must be due to new layers being nucleated during dewetting. (The disappearance of some very small islands in Figs. 2(a) and 2(b) could also be due to sublimation.)

It is difficult to observe individual nucleation events directly because the sample must be quenched to <120 K for nondestructive imaging. However, by scanning with sample voltages $|V_{\text{sample}}| < 5$ V several uppermost H_2O layers can be removed with the STM tip, thus creating very flat crystals for which the driving force of dewetting is extremely high. Then, after switching to imaging mode, i.e., increasing the sample bias to $|V_{\text{sample}}| > 5$ V, we are able to observe [Figs. 2(c) and 2(d)] the formation of triangular nuclei, which readily expand until they cover the entire crystal even at 120 K.

To analyze these data we adapt the approach of Mullins and Rohrer to the dewetting case. First consider the driving force. Assume that the ice crystals are strain free [14,15] hexagonal prisms of height h and prism length R. Assume further that the volume, Ω, per water molecule is approximately the same for the wetting layer and the crystal. The supersaturation of admolecules on top of the basal surface of the crystallites is determined by the decrease in free energy that occurs when molecules are removed from the prism faces of the crystals, increasing the area covered by the wetting layer. The corresponding chemical potential, relative to bulk ice, is a sum of contributions from changing the areas of the horizontal basal and vertical prism faces of the crystallites:

$$\mu = \Omega(\gamma_b + \gamma_{\text{ice-Pt}} - \gamma_{\text{wetting}})/h + 2\Omega\gamma_p/(\sqrt{3}R). \quad (1)$$

Here γ_b is the basal plane surface free energy per unit area, γ_p is the surface free energy of the prism faces, $\gamma_{\text{ice-Pt}}$ is the free energy/area of the ice-Pt interface, and γ_{wetting} is the specific free energy of the Pt surface covered by the wetting layer. The driving force μ for dewetting decreases as the crystals become higher because the change in interfacial area per water molecule decreases as $1/h$.

Given this driving force we use standard nucleation theory to calculate the rate J for nucleating triangular islands as observed on top of the hexagonal prisms. The free energy G of a triangular island of side length r, subject to the chemical potential μ given by Eq. (1) is $G(r) = 3\beta r - \frac{\sqrt{3}}{4}\frac{h_0}{\Omega}\mu r^2$, where h_0 is the height and β the energy per length of the molecular step that bounds the nucleated layer. The maximum of $G(r)$ yields the critical size $r_c = 2\sqrt{3}\frac{\Omega\beta}{\mu h_0}$. Assuming that the nucleation rate is proportional to the thermal probability of creating a critical nucleus, i.e., $J \propto \exp[-G(r_c)/kT]$, we find the island nucleation rate J in our limit of $R \gg h$ decreases exponentially with h:

$$J(h) \propto \exp\left[-\frac{1}{\gamma_b + \gamma_{\text{ice-Pt}} - \gamma_{\text{wetting}}}\frac{3\sqrt{3}\beta^2}{kT}\frac{h}{h_0}\right]. \quad (2)$$

We now compare to our experimental data. Figure 3(c) displays how often crystallites were observed to change their height by n layers during the 1 h anneal, for various starting heights. Clearly there is a correlation between height and growth rate—lower-height crystallites nucleate new layers more quickly, as expected from the theory. Figure 3(d) shows what Eq. (2) predicts for the crystal height changes between Figs. 2(a) and 2(b), along with the calculated statistical standard deviations. To construct this figure we fit the height changes observed for crystals of height 6 to obtain values of $J(6)$ and of the exponential factor in Eq. (2). With no further fitting, we then reproduce within statistical errors the rates of height changes for crystals 5 and 7 layers high [22]. From this fit one can estimate that $3\sqrt{3}\beta^2/[(\gamma_b + \gamma_{\text{ice-Pt}} - \gamma_{\text{wetting}})kT] \approx \ln(2.5) \approx 1$ for ice at 140 K.

The exponential decrease of the nucleation rate with height determines the film morphology: For crystallites of fewer than 5 layers, nucleation is fast enough that they all grow higher than 4 layers already during the deposition. (Here, of course, the deposition flux enhances the nucleation.) On the other hand, nucleation on top of crystallites more than 10 layers high becomes so slow as to be hard to observe, even though the ice crystals are still much flatter than in equilibrium. These results also imply that dewetting is dominated by the rearrangement of material within crystals and not between them (i.e., not by Ostwald ripening). In the case of Ostwald ripening (where the super-

saturation on each crystal is the same and determined by the average crystal size), nucleation would have been proportional to the area of a crystal's top facet but independent of the crystal's height.

Lastly, we note that the energies extracted from our fits to nucleation data permit inferences concerning the energetics of ice steps and interfaces and their molecular structure. We first define two energies per area that measure the interactions with the substrate of (i) the wetting layer and (ii) an ice crystal. We take $\varepsilon_{\text{Pt-ice}}$ to be the energy decrease per area when the basal plane of a macroscopic ice crystal is placed in contact with the substrate, i.e., $\gamma_{\text{Pt-ice}} = \gamma_{\text{Pt}} + \gamma_b - \varepsilon_{\text{Pt-ice}}$. Then we define an analogous quantity $\varepsilon_{\text{wetting}}$ for the wetting layer by comparing its energetics to a bulk-ice crystal with two surfaces that is brought into contact with the Pt substrate: i.e., $\gamma_{\text{wetting}} = \gamma_{\text{Pt}} + 2\gamma_b - \varepsilon_{\text{wetting}}$. Accordingly, we rewrite the estimate above as

$$\left(\frac{\varepsilon_{\text{wetting}} - \varepsilon_{\text{Pt-ice}}}{\gamma_b}\right)\left(\frac{a\gamma_b}{\beta}\right)^2 \approx \left(\frac{3\sqrt{3}a^2}{kT}\gamma_b\right), \qquad (3)$$

where we introduce the distance $a = 0.45$ nm, the separation between equivalent O atoms at a molecular step, to make each factor in the equation dimensionless. Experimental data and counting the hydrogen bonds broken to create a basal surface of ice suggest that γ_b is within a factor of 2 of 100 mJ/m^2 [1], which yields an estimate of 20 for the right-hand side of Eq. (3) at 140 K. Ignoring surface relaxations and reconstructions, we model the surface and steps as truncated bulk ice with energies proportional to the number of broken nearest neighbor "bonds." In this model the equilibrium island shape is triangular, consistent with our observations, with a step edge energy of $\beta = a\gamma_b/\sqrt{3}$. Substituting this result into Eq. (3) would imply that $\varepsilon_{\text{ice-Pt}} - \varepsilon_{\text{wetting}} \approx 7\gamma_b$. Such a large difference between $\varepsilon_{\text{ice-Pt}}$ and $\varepsilon_{\text{wetting}}$ is unreasonable if, as expected, the main difference between the ice in the wetting layer and at the ice-Pt interfaces lies in the different arrangement of hydrogen bonds. For example, it has been proposed [3,4,12,15] that in the wetting layer there are no broken hydrogen bonds pointing away from the substrate, as there are at the surface of truncated bulk ice. From this sort of bonding rearrangement we expect $\varepsilon_{\text{ice-Pt}} - \varepsilon_{\text{wetting}}$ to be on the order of γ_b—but not 7 times γ_b—and argue that simple bond counting overestimates the step energies on ice by at least a factor of 3, suggesting significant relaxations or a reconstruction of the step edge. However, even with such a reduction in β, our results still suggest that $\varepsilon_{\text{ice-Pt}} - \varepsilon_{\text{wetting}}$ is a considerable fraction of γ_b, indicating significant structural differences between how the wetting layer and bulk ice are bound to Pt.

In summary, we have shown that ice crystals, growing one molecular layer at a time, can be imaged with STM. The promise of this advance is demonstrated by the fact that we have observed and characterized the nucleation of molecular layers of ice on ice. From our analysis of the observed nucleation rates we have deduced that the step energies on ice are considerably smaller than predicted from bond counting arguments, and that the difference between the bonding of the wetting layer and the bulk-ice Pt interface is on the order of the ice-vacuum surface energy. The driving force for dewetting of ice on Pt(111) is strong enough to cause nucleation of new layers, which slows down as the crystallites become higher. Although understanding dewetting-induced nucleation is crucial for predicting the stability of thin films, it has not been quantified before in any system.

We are grateful to P. J. Feibelman for valuable discussions. This research was supported by the Office of Basic Energy Sciences, Division of Materials Sciences, U. S. Department of Energy under Contracts No. DEAC04-94AL85000.

[1] V. F. Petrenko and R. W. Whitworth, *Physics of Ice* (Oxford University Press, Oxford, 1999).
[2] F. C. Frank, Contemp. Phys. **23**, 3 (1982).
[3] P. J. Feibelman, Science **295**, 99 (2002); Phys. Rev. Lett. **91**, 059601 (2003).
[4] A. Verdaguer *et al.*, Chem. Rev. **106**, 1478 (2006).
[5] M. Mehlhorn and K. Morgenstern, Phys. Rev. Lett. **99**, 246101 (2007).
[6] M. Morgenstern *et al.*, Z. Phys. Chem. **198**, 43 (1997).
[7] A. Michaelides and K. Morgenstern, Nat. Mater. **6**, 597 (2007).
[8] E. Jiran and C. V. Thompson, J. Electron. Mater. **19**, 1153 (1990).
[9] O. Pierre-Louis, A. Chame, and Y. Saito, Phys. Rev. Lett. **99**, 136101 (2007).
[10] K. Thürmer, E. D. Williams, and J. E. Reutt-Robey, Phys. Rev. B **68**, 155423 (2003).
[11] W. L. Ling *et al.*, Surf. Sci. **570**, L297 (2004).
[12] G. A. Kimmel *et al.*, J. Chem. Phys. **126**, 114702 (2007).
[13] M. A. Henderson, Surf. Sci. Rep. **46**, 1 (2002).
[14] S. Haq, J. Harnett, and A. Hodgson, Surf. Sci. **505**, 171 (2002).
[15] A. Glebov *et al.*, J. Chem. Phys. **106**, 9382 (1997); **112**, 11 011 (2000).
[16] N. Materer *et al.*, Surf. Sci. **381**, 190 (1997).
[17] W. W. Mullins and G. S. Rohrer, J. Am. Ceram. Soc. **83**, 214 (2000).
[18] K. Thürmer, J. E. Reutt-Robey, and E. D. Williams, Surf. Sci. **537**, 123 (2003).
[19] W. Ranke, Surf. Sci. **209**, 57 (1989).
[20] K. Thürmer and N. C. Bartelt [Phys. Rev. B (to be published)].
[21] See EPAPS Document No. E-PRLTAO-100-013817 for an STM image of the wetting layer and gray scale versions of Figs. 2(a) and 2(b). For more information on EPAPS, see http://www.aip.org/pubservs/epaps.html.
[22] Presumably J is proportional to the area of the crystallites. However, the relatively sharp experimental distribution of areas allows us to neglect this effect.